Mathematical Methods in Medical Image Processing and Magnetic Resonance Imaging

Joyjit patra[1], Himadri Nath Moulick[2], Arun Kanti Manna[3], Rajarshi Roy[4]
[1](C.S.E, Aryabhatta Institute Of Engineering And Management,Durgapur,West Bengal,India)
[2](C.S.E, Aryabhatta Institute Of Engineering And Management,Durgapur,West Bengal,India)
[3](Persuing Ph.D. from Techno India University,W.B.India)
[4](B.Tech 4th year Student,CSE Dept,Aryabhatta Institute of Engineering and Mangement,Durgapur,W.B,India)

ABSTRACT:
In this paper,we describe some central mathematical problems in medical imaging.The subject has been undergoing rapid changes driven by better hardware and software.Much of the software is based on novel methods utilizing geometric partial differential equations in conjunction with standard signal/image processing techniques as well as computer graphics facilitating man/machine interactions.As part of this enterprise,researchers have been trying to base biomedical engineering principles on rigorous mathematical foundations for the development of software methods to be integrated into complete therapy delivery systems.These systems support the more effective delivery of many image-guided procedures such as radiation therapy,biopsy,and minimally invasive surgery.We will show how mathematics may impact some of the main problems in this area including image enhancement,registration,and segmentation.This paper[1] describes image processing techniques for Diffusion Tensor Magnetic Resonance.In Diffusion Tensor MRI,a tensor describing local water diffusion is acquired for each voxel. The geometric nature of the diffusion tensors can quantitatively characterize the local structure in tissues such as bone,muscles,and white matter of the brain.The close relationship between local image structure and apparent diffusion makes this image modality very interesting for medical image analysis.We present a decomposition of the diffusion tensor based on its symmetry properties resulting in useful measures describing the geometry of the diffusion ellipsoid. A simple anisotropy measure follows naturally from this analysis.We describe how the geometry,or shape,of the tensor can be visualized using a coloring scheme based on the derived shape measures.We show how filtering of the tensor data of a human brain can provide a description of macrostructural diffusion which can be used for measures of fiber-tract organization.We also describe how tracking of white matter tracts can be implemented using the introduced methods.

Keywords: *Medical imaging, artificial vision, smoothing, registration, segmentation, image-guided therapy (IGT) and image guided surgery (IGS).*

I. INTRODUCTION

Medical imaging has been undergoing a revolution in the past decade with the advent of faster, more accurate,and less invasive devices.This has driven the need for corresponding software development which in turn has provided a major impetus for new algorithms in signal and image processing. Many of these algorithms are based on partial differential equations and curvature driven flows which will be the main topics of this survey paper.Mathematical models are the foundation of biomedical computing.Basing those models on data extracted from images continues to be a fundamental technique for achieving scientific progress in experimental,clinical,biomedical,and behavioral research.Today,medical images are acquired by a range of techniques across all biological scales,which go far beyond the visible light photographs and microscope images of the early 20th century.Modern medical images may be considered to be geometrically arranged arrays of data samples which quantify such diverse physical phenomena as the time variation of hemoglobin deoxygenation during neuronal metabolism,or the diffusion of water molecules through and within tissue.The broadening scope of imaging as a way to organize our observations of the biophysical world has led to a dramatic increase in our ability to apply new processing techniques and to combine multiple channels of data into sophisticated and complex mathematical models of physiological function and dysfunction.A key research area is the formulation of biomedical engineering principles based on rigorous mathematical foundations in order to develop general-purpose software methods that can be integrated into complete therapy delivery systems.Such systems support the more effective delivery of many image-guided procedures such as biopsy,minimally invasive surgery,and radiation therapy.In order to understand the extensive role of imaging in the therapeutic process, and to appreciate the current usage of images before,during,and after treatment,we focus our analysis on four main components of image-guided therapy (IGT) and image guided surgery (IGS): localization, targeting, monitoring, and control.Specifically, in medical imaging we have four key problems:

(1)Segmentation- automated methods that create patient-specific models of relevant anatomy from images;(2) Registration - automated methods that align multiple data sets with each other;(3) Visualization - the technological environment in which image-guided procedures can be displayed;(4) Simulation - softwares that can be used to rehearse and plan procedures,evaluate access strategies, and simulate planned treatments.In this paper,we will only consider the first two problem areas. However,it is essential to note that in modern medical imaging,we need to integrate these technologies into complete and coherent image guided therapy delivery systems and validate these integrated systems using performance measures established in particular application areas.We should note that in this survey we touch only upon those aspects of the mathematics of medical imaging reflecting the personal tastes (and prejudices) of the authors.Indeed,we do not discuss a number of very important techniques such as wavelets,which have had a significant impact on imaging and signal processing; see [60] and the references therein. Several articles and books are available which describe various mathematical aspects of imaging processing such as [67] (segmentation), [83] (curve evolution), and [71, 87] (level set methods).Finally,it is extremely important to note that all the mathematical algorithms which we sketch lead to interactive procedures.This means that in each case there is a human user in the loop (typically a clinical radiologist) who is the ultimate judge of the utility of the procedure, and who tunes the parameters either on or off-line. Nevertheless, there is a major need for further mathematical techniques which lead to more automatic and easier to use medical procedures. We hope that this paper may facilitate a dialogue between the mathematical and medical imaging communities.Diffusion Tensor Magnetic Resonance Imaging (DT-MRI) is a recent MR imaging modality. In Diffusion Tensor MRI, a tensor describing local water diffusion is acquired for each voxel. Diffusion in tissue can be anisotropic depending on the characteristics of the tissue. For example in the white matter fiber tracts the diffusion is mainly in the direction of the fibers. In areas with fluid, such in the CSF filled ventricles, the diffusion is spherical, i.e. isotropic. The advent of robust diffusion tensor imaging techniques has prompted the development of quantitative measures for describing the diffusion anisotropy. A good review by Basser and Pierpaoli can be found in [1]. Since MRI methods in general always obtain a macroscopic measure of a microscopic quantity which necessarily entails intravoxel averaging, the voxel dimensions influence the measured diffusion tensor at any particular location in the brain. Factors which would affect the shape of the apparent diffusion tensor (shape of the diffusion ellipsoid) in the white matter include the density of fibers, the degree of myelination, the average fiber diameter and the directional similarity of the fibers in the voxel. The geometric nature of the measured diffusion tensor within a voxel is thus a meaningful measure of fiber tract organization.With current conventional proton magnetic resonance imaging (MRI) techniques, the white matter of the brain appears to be a remarkably homogeneous tissue without any suggestion of the complex arrangement of fiber tracts. Although the individual axons and the surrounding myelin sheaths cannot be revealed with the limited spatial resolution of in vivo imaging, distinct bands of white matter fibers with parallel orientation may be distinguished from others running in different directions if MRI techniques are sensitized to water diffusion and the preferred direction of diffusion is determined.Water diffusion in tissue due to Brownian motion is random but some structural characteristics of tissues may limit diffusion.In the white matter, the mobility of the water is restricted in the directions perpendicular to the axons which are oriented along the fiber tracts. This anisotropic diffusion is due to the presence of tightly packed multiple myelin membranes encompassing the axon. Myelination is not essential for diffusion anisotropy of nerves as shown in studies of nonmyelinated garfish olfactory nerves [3] and anisotropy exists in brains of neonates before the histological appearance of myelin [16] but myelin is widely assumed to be the major barrier to diffusion in myelinated fiber tracts. Therefore the demonstration of anisotropic diffusion in brain by magnetic resonance has opened the way to explore noninvasively the structural anatomy of the white matter in vivo [8, 4, 1, 10].

II. MEDICAL IMAGING

2.1. Generalities

In 1895, Roentgen discovered X-rays and pioneered medical imaging.His initial publication [82] contained a radiograph (i.e. an X-ray generated photograph) of Mrs. Roentgen's hand; see Figure1(a).For the first time, it was possible to visualize non-invasively (i.e., not through surgery) the interior of the human body.The discovery was widely publicized in the popular press and an "Xray mania" immediately seized Europe and the United States [30, 47]. Within only a few months, public demonstrations were organized, commercial ventures created and innumerable medical applications investigated; The field of radiography was born with a bang!Today,medical imaging is a routine and essential part of medicine. Pathologies can be observed directly rather than inferred from symptoms.For example, a physician can non-invasively monitor the healing of damaged tissue or the growth of a brain tumor, and determine an appropriate medical response. Medical imaging techniques can also be used when planning or even while performing surgery. For

(a) First radiograph of Mrs. Roentgen's hand.
Fig:1. X-ray radiography at the end of the 19th century.

example,a neurosurgeon can determine the "best" path in which to insert a needle,and then verify in real time its position as it is being inserted.

III. MAGNETIC RESONANCE IMAGING

This technique relies on the relaxation properties of magnetically-excited hydrogen nuclei of water molecules in the body.The patient under study is briefly exposed to a burst of radio-frequency energy,which,in the presence of a magnetic field,puts the nuclei in an elevated energy state.As the molecules undergo their normal,microscopic tumbling, they shed this energy into their surroundings, in a process referred to as relaxation.Images are created from the difference in relaxation rates in different tissues.This technique was initially known as nuclear magnetic resonance (NMR) but the term "nuclear" was removed to avoid any association with nuclear radiation.MRI utilizes strong magnetic fields and non-ionizing radiation in the radio frequency range,and according to current medical knowledge,is harmless to patients.Another advantage of MRI is that soft tissue contrast is much better than with X-rays leading to higher-quality images, especially in brain and spinal cord scans.See Figure 2(a). Refinements have been developed such as functional MRI (fMRI) that measures temporal variations (e.g., for detection of neural activity), and diffusion MRI that measures the diffusion of water molecules in anisotropic tissues such as white matter in the brain.

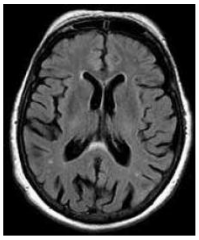

Fig: 2(a).Magnetic Resonance Image(brain, 2D axial slice).

IV. POSITRON EMISSION TOMOGRAPHY

The patient is injected with radioactive isotopes that emit particles called positrons (anti-electrons).When a positron meets an electron,the collision produces a pair of gamma ray photons having the same energy but moving in opposite directions.From the position and delay between the photon pair on a receptor, the origin of the photons can be determined. While MRI and CT can only detect anatomical changes,PET is a functional modality that can be used to visualize pathologies at the much finer molecular level.Ths is achieved by employing radioisotopes that have different rates of intake for different tissues.For example,the change of regional blood flow in various anatomical structures (as a measure of the injected positron emitter) can be visualized and relatively quantified.Since the patient has to be injected with radioactive material,PET is relatively invasive.The radiation dose however is similar to a CT scan.Image resolution may be poor and major preprocessing may be necessary.See Figure 3(a).

Figure 3(a). Positron Emission Tomography(brain, 2D axial slice).

V. ALGORITHMS & PDES

Many mathematical approaches have been investigated for applications in artificial vision(e.g.,fractals and self-similarity,wavelets,pattern theory,stochastic point process,random graph theory; see [42]).In particular,methods based on partial differential equations (PDEs) have been extremely popular in the past few years [20, 35].Here we briefly outline the major concepts involved in using PDEs for image processing.As explained in detail in [17], one can think of an image as a map I : D → C, i.e., to any point x in the domain D, I associates a "color" I(x) in a color space C. For ease of presentation we will mainly restrict ourselves to the case of a twodimensional gray scale image which we can think of as a function from a domain D = [0, 1] × [0, 1] to the unit interval C = [0, 1].The algorithms all involve solving the initial value problem for some PDE for a given amount of time. The solution to this PDE can be either the image itself at different stages of modification, or some other object (such as a closed curve delineating object boundaries) whose evolution is driven by the image. For example, introducing an artificial time t, the image can be deformed according to

$$\frac{\partial I}{\partial t} = \mathcal{F}[I], \qquad \text{.....(1)}$$

where I(x, t) : D × [0, T) → C is the evolving image,F is an operator which characterizes the given algorithm, and the initial condition is the input image I0.The processed image is the solution I(x, t) of the differential equation at time t.The operator F usually is a differential operator, although its dependence on I may also be nonlocal.Similarly,one can evolve a closed curve representing the boundaries of some planar shape (Γ need not be connected and could have several components).In this case, the operator F specifies the normal velocity of the curve that it deforms. In many cases this normal velocity is a function of the curvature κ of Γ ,and of the image I evaluated on Γ .A flow of the form

$$\frac{\partial \Gamma}{\partial t} = \mathcal{F}(I, \kappa)\mathbf{N} \qquad \text{.....(2)}$$

is obtained,where N is the unit normal to the curve Γ .Very often,the deformation is obtained as the steepest descent for some energy functional.For example,the energy

$$\mathcal{E}(I) = \frac{1}{2}\int \|\nabla I\|^2 \, dxdy \qquad \text{.....(3)}$$

and its associated steepest descent, the heat equation,

$$\frac{\partial I}{\partial t} = \Delta I \qquad \text{.....(4)}$$

correspond to the classical Gaussian smoothing.The use of PDEs allows for the modelling of the crucial but poorly understood interactions between top-down and bottom-up vision 5.In a variational framework, for example, an energy $\mathcal{E}$ is defined globally while the corresponding operator F will influence the image locally.Algorithms defined in terms of PDEs treat images as continuous rather than discrete objects.This simplifies the formalism,which becomes grid independent.On the other hand models based on nonlinear PDEs may be much harder to analyze and implement rigorously.

VI. IMAGING PROBLEMS

Medical images typically suffer from one or more of the following imperfections:

- low resolution (in the spatial and spectral domains);
- high level of noise;
- low contrast;
- geometric deformations;
- presence of imaging artifacts.

These imperfections can be inherent to the imaging modality (e.g.,X-rays offer low contrast for soft tissues,ultrasound produces very noisy images,and metallic implants will cause imaging artifacts in MRI) or the result of a deliberate trade-off during acquisition.For example,finer spatial sampling may be obtained through a longer acquisition time.However that would also increase the probability of patient movement and thus blurring.In this paper,we will only be interested in the processing and analysis of images and we will not be concerned with the challenging problem of designing optimal procedures for their acquisition.Several tasks can be performed(semi)-automatically to support the eye-brain system of medical practitioners.Smoothing is the problem of simplifying the image while retaining important information. Registration is the problem of fusing images of the same region acquired from different modalities or putting in correspondence images of one patient at different times or of different patients.Finally,segmentation is the problem of isolating anatomical structures for quantitative shape analysis or visualization.The ideal clinical application should be fast,robust with regards to image imperfections, simple to use,and as automatic as possible.The ultimate goal of artificial vision is to imitate human vision,which is intrinsically subjective.The technique we present below are applied to two-dimensional grayscale images.The majority of them,however,can be extended to higher dimensions(e.g., vector-valued volumetric images).

6.1. Image Segmentation

When looking at an image, a human observer cannot help seeing structures which often may be identified with objects. However,digital images as the raw retinal input of local intensities are not structured. Segmentation is the process of creating a structured visual representation from an unstructured one.The problem was first studied in the 1920's by psychologists of the Gestalt school (see Kohler [54] and the references therein),and later by psychophysicists [49, 95].In its modern formulation,image segmentation is the problem of partitioning an image into homogeneous regions that are semantically meaningful,i.e.,that correspond to objects we can identify.Segmentation is not concerned with actually determining what the partitions are. In that sense,it is a lower level problem than object recognition.In the context of medical imaging,these regions have to be anatomically meaningful.A typical example is partitioning a MRI image of the brain into the white and gray matter.Since it replaces continuous intensities with discrete labels,segmentation can be seen as an extreme form of smoothing/information reduction. Segmentation is also related to registration in the sense that if an atlas can be perfectly registered to a dataset at hand,then the registered atlas labels are the segmentation.Segmentation is useful for visualization,it allows for quantitative shape analysis,and provides an indispensable anatomical framework for virtually any subsequent automatic analysis.Indeed, segmentation is perhaps the central problem of artificial vision,and accordingly many approaches have been proposed (for a nice survey of modern segmentation methods,see the monograph [67]).There are basically two dual approaches.In the first, one can start by considering the whole image to be the object of interest,and then refine this initial guess.These "split and merge"techniques can be thought of as somewhat analogous to the top-down processes of human vision. In the other approach,one starts from one point assumed to be inside the object,and adds other points until the region encompasses the object.Those are the "region growing"techniques and bear some resemblance to the bottom-up processes of biological vision.The dual problem to segmentation is that of determining the boundaries of the segmented homogeneous regions.This approach has been popular for some time since it allows one to build upon the well-investigated problem of edge detection(Section 6.2).Difficulties arise with this approach because noise can be responsible for spurious edges. Another major difficulty is that local edges need to be connected into topologically correct region boundaries.To address these issues,it was proposed to set the topology of the boundary to that of a sphere and then deform the geometry in a variational framework to match the edges.In 2D,the boundary is a closed curve and this approach was named snakes. Improvements of the technique include geometric active contours and conformal active contours.All these techniques are generically referred to as active contours.Finally,as described in [67], most segmentation methods can be set in the elegant mathematical framework proposed by Mumford and Shah [69].

6.2. Edge Detectors

Consider the ideal case of a bright object $\mathcal{O}$ on a dark background.The physical object is represented by its projections on the image I.The characteristic function $1_{\mathcal{O}}$ of the object is the ideal segmentation, and since the object is contrasted on the background, the variations of the intensity I are large on the boundary $\partial\mathcal{O}$.It is therefore natural to characterize the boundary $\partial\mathcal{O}$ as the locus of points where the norm of the gradient |I| is large.In fact, if $\partial\mathcal{O}$ is piecewise smooth then |I| is a singular measure whose support is exactly $\partial\mathcal{O}$.This is the approach taken in the 60's and 70's by Roberts [81] and Sobel [91] who proposed slightly different discrete convolution masks to approximate the gradient of digital images.Disadvantages with these approaches are that edges are not precisely localized, and may be corrupted by noise. See Figure 4(b) is the result of a Sobel edge detector on a medical image.Note the thickness of the boundary of the heart ventricle as well as the presence of "spurious edges" due to noise. Canny [14] proposed to add a smoothing pre-processing step (to reduce the influence of the noise) as well as a thinning post-processing phase (to ensure that the edges are uniquely localized).See [26] for a survey and evaluation of edge detectors using gradient techniques.A slightly different approach initially motivated by psychophysics was proposed by Marr and Hildreth [62, 61] where edges are defined as the zeros of $\Delta G_\sigma * I$, the Laplacian of a smooth version of the image.One can give a heuristic justification by assuming that the edges are smooth curves; more precisely,assume that near

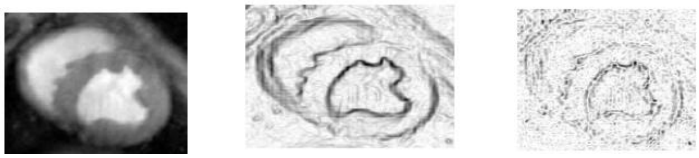

(a) Original image b) Sobel edge detector c) Marr edge detector.

Fig.4 Result of two edge detectors on a heart MRI image.

an edge the image is of the form

$$I(\boldsymbol{x}) = \varphi\left(\frac{S(\boldsymbol{x})}{\varepsilon}\right), \quad \text{.....(5)}$$

where S is a smooth function which vanishes on the edge, ε is a small parameter proportional to the width of the edge, and R → [0, 1] is a smooth increasing function with limits.

Fig. 4.1.

VII. MATERIALS AND METHODS

In this work we applied a modified version of the recently proposed Line Scan Diffusion Imaging (LSDI) technique.This method, like the commonly used diffusionsensitized,ultrafast, echo-planar imaging (EPI) technique [12] is relatively insensitive to bulk motion and physiologic pulsations of vascular origin.But unlike EPI,LSDI exhibits minimal image distortion,does not require cardiac gating,head restraints or post-processing image correction,and can be implemented without specialized hardware on all standard MRI scanners.Here,we present a quantitative characterization of the geometric nature of the diffusiontensors,a method for characterization of marcostructural diffusion properties,and a display method for showing clear and detailed in vivo images of human white mattertracts.The orientation and distribution of most of the known major fiber tracts can be identified using these methods.

7.1. Imaging Parameters

Suppose, some data were acquired at a hospital on a GE Signa 1.5 Tesla,Horizon Echospeed 5.6 system with standard 2.2 Gauss/cm field gradients.The time required for acquisition of the diffusion tensor data for one slice was 1 min;no averaging was performed. Imaging parameters were:effective TR=2.4 s, TE=65 b_{high}=750 s/b_{low}=5 s/mm^2,field of view 22 cm, effective voxel size 4.8_1.6_1.5 mm3,6 kHz readout bandwidth, acquisition matrix 128_128.The gradient cycle in the LSDI interleaving scheme was modified to provide acquisition of more gradient directions and to allow elimination of the crusher gradients. Instead of alternating merely between high and low gradient strengths, the modified sequence cycled through eight configurations of the diffusion gradients.In all other respects it was identical to the sequence described in [7].

7.2. Calculation of Tensors

For each slice, eight images are collected with different diffusion weightings and noncollinear gradient directions. If S_0 represents the signal intensity in the absence of a diffusion-sensitizing field gradient and S the signal intensity in the presence of gradient $\mathbf{g} = (g_x, g_y, g_z)$,the equation for the loss in signal intensity due to diffusion is given by the Stejskal-Tanner formula:

$$\ln(S) = \ln(S_0) - \gamma^2\delta^2(\Delta - \delta/3)\mathbf{g}^T\mathbf{D}\mathbf{g}, \quad \text{.....(6)}$$

where γ is the gyromagnetic ratio of hydrogen 1H (protons), δ is the duration of the diffusion sensitizing gradient pulses and Δ is the time between the centers of the two gradient pulses. The eight images provide eight equations for S in each voxel which are solved in a least-squares sense for the 6+1 unknowns: the six independent components of the symmetric diffusion tensor, $\mathbf{D}$,and S_0.In the LSDI sequence, it is easy to show that cross terms between the slice select gradient for the 180 pulse and the diffusion sensitizing gradients account for less than 0.1% of the diffusion weighting,and have therefore been neglected here.Diffusion attenuation due to imaging gradients is already factored into S_0 ,as is T2 weighting.

7.3. Geometrical Measures of Diffusion

In order to relate the measure of diffusion anisotropy to the structural geometry of the tissue a mathematical description of diffusion tensors and their quantification is necessary. First, a complete diffusion tensor, D, is calculated for each voxel. Using the symmetry properties of the diffusion ellipsoid we decomposed the diffusion tensor, and from the tensor basis assigned scalar measures, describing the linearity and the anisotropy, to each voxel. The diffusion tensor can be visualized using an ellipsoid where the principal axes correspond to the directions of the eigenvector system. Let $\lambda_1 \geq \lambda_2 \geq \lambda_3 \geq 0$ be the eigenvalues of the symmetric tensor D

$$\mathbf{D} = \lambda_1\hat{\mathbf{e}}_1\hat{\mathbf{e}}_1^T + \lambda_2\hat{\mathbf{e}}_2\hat{\mathbf{e}}_2^T + \lambda_3\hat{\mathbf{e}}_3\hat{\mathbf{e}}_3^T \quad \text{.....(7)}$$

Diffusion can be divided into three basic cases depending on the rank, of the representation tensor:

1) Linear case $(\lambda_1 \gg \lambda_2 \simeq \lambda_3)$: diffusion is mainly in the direction corresponding to the largest eigenvalue.

$$\mathbf{D} \simeq \lambda_1\mathbf{D}_l = \lambda_1\hat{\mathbf{e}}_1\hat{\mathbf{e}}_1^T. \quad \text{.....(8)}$$

2) Planar case $(\lambda_1 \simeq \lambda_2 \gg \lambda_3)$: diffusion is restricted to a plane spanned by the two eigenvectors corresponding to the two largest eigenvalues.

$$\mathbf{D} \simeq 2\lambda_1\mathbf{D}_p = \lambda_1(\hat{\mathbf{e}}_1\hat{\mathbf{e}}_1^T + \hat{\mathbf{e}}_2\hat{\mathbf{e}}_2^T). \quad \text{.....(9)}$$

3) Spherical case $(\lambda_1 \simeq \lambda_2 \simeq \lambda_3)$isotropic diffusion:

$$\mathbf{D} \simeq 3\lambda_1\mathbf{D}_s = \lambda_1(\hat{\mathbf{e}}_1\hat{\mathbf{e}}_1^T + \hat{\mathbf{e}}_2\hat{\mathbf{e}}_2^T + \hat{\mathbf{e}}_3\hat{\mathbf{e}}_3^T). \quad \text{....(10)}$$

In general, the diffusion tensor D will be a combination of these cases. Expanding the diffusion tensor using these cases as a basis gives:

$$\begin{aligned}\mathbf{D} &= \lambda_1\hat{\mathbf{e}}_1\hat{\mathbf{e}}_1^T + \lambda_2\hat{\mathbf{e}}_2\hat{\mathbf{e}}_2^T + \lambda_3\hat{\mathbf{e}}_3\hat{\mathbf{e}}_3^T \\ &= (\lambda_1 - \lambda_2)\hat{\mathbf{e}}_1\hat{\mathbf{e}}_1^T + (\lambda_2 - \lambda_3)(\hat{\mathbf{e}}_1\hat{\mathbf{e}}_1^T + \hat{\mathbf{e}}_2\hat{\mathbf{e}}_2^T) \\ &\quad + \lambda_3(\hat{\mathbf{e}}_1\hat{\mathbf{e}}_1^T + \hat{\mathbf{e}}_2\hat{\mathbf{e}}_2^T + \hat{\mathbf{e}}_3\hat{\mathbf{e}}_3^T) \\ &= (\lambda_1 - \lambda_2)\mathbf{D}_l + (\lambda_2 - \lambda_3)\mathbf{D}_p + \lambda_3\mathbf{D}_s \quad \text{.....(11)}\end{aligned}$$

where $(\lambda_1 - \lambda_2)$, $(\lambda_2 - \lambda_3)$ and λ_3 are the coordinates of D in the tensor basis $\{\mathbf{D}_l, \mathbf{D}_p, \mathbf{D}_s\}$ .A similar tensor shape analysis has proven to be useful in a number of computer vision applications.As described,the relationships between the eigenvalues of the diffusion tensor can be used for classification of the diffusion tensor according to geometrically meaningful criteria.By using the coordinates of the tensor in our new basis measures are obtained of how close the diffusion tensor is to the generic cases of line,plane and sphere.The generic shape of a tensor is obtained by normalizing with a magnitude measure of the diffusion.Here we define this magnitude as the largest eigenvalues of the tensor.This gives for the linear, planar and spherical measures:

$$c_l = \frac{\lambda_1 - \lambda_2}{\lambda_1}$$

$$c_p = \frac{\lambda_2 - \lambda_3}{\lambda_1}$$

$$c_s = \frac{\lambda_3}{\lambda_1}$$

$$c_l + c_p + c_s = 1 \quad \text{.....(12)}$$

An anisotropy measure describing the deviation from the spherical case is achieved as follows:

$$c_a = c_l + c_p = 1 - c_s = 1 - \frac{\lambda_3}{\lambda_1} \quad \text{.....(13)}$$

7.4. Visualization of Diffusion Tensors

A 3D diffusion tensor can be visualized using an ellipsoid where the principal axes correspond to the tensor's eigenvector system. However,it is difficult to distinguish between an edge-on, flat ellipsoid and an oblong one using the surface shading information.Similar ambiguity exists between a face-on,flat ellipsoid and a sphere.We propose two techniques for the visualization of tensor fields that overcome the problems with ellipsoids.We compares the ellipsoidal representation of a tensor with a composite shape whose linear,planar,and spherical components are scaled according to c_l, c_p, and c_s (cl, cp, and cs).Additionally,coloring based on the shape measures c_l, c_p, and c_s can be used for visualization of shape.

VIII. CONCLUSION

In this paper,we sketched some of the fundamental concepts of medical image processing.It is important to emphasize that none of these problem areas has been satisfactorily solved,and all of the algorithms we have described are open to considerable improvement. In particular,segmentation remains a rather ad hoc procedure with the best results being obtained via interactive programs with considerable input from the user.Nevertheless,progress has been made in the field of automatic analysis of medical images over the last few years thanks to improvements in hardware,acquisition methods,signal processing techniques,and of course mathematics.Curvature driven flows have proven to be an excellent tool for a number of image processing tasks and have definitely had a major impact on the technology base.Several algorithms based on partial differential equation methods have been incorporated into clinical software and are available in open software packages such as the National Library of Medicine Insight Segmentation and Registration Toolkit (ITK), and the 3D Slicer of the Harvard Medical School [90].These projects are very important in disseminating both standard and new mathematical methods in medical imaging to the broader community.

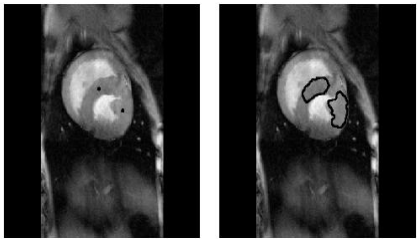

(a)Two initial bubbbles. (b) Evolving active contours

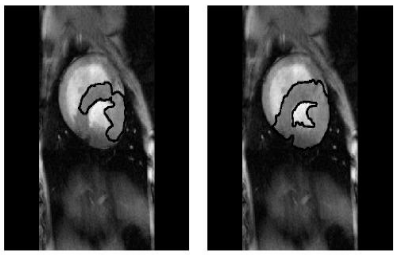

(c) Merging of active contours. (d) Steady state.

Fig.5 Myocardium segmentation in MRI heart image with two merging expanding conformal active contours.

The mathematical challenges in medical imaging are still considerable and the necessary techniques touch just about every major branch of mathematics.In summary,we can use all the help we can get!We have proposed measures classifying diffusion tensors into three generic cases based on a tensor basis expansion.When applied to white matter the linear index shows uniformity of tract direction within a voxel while the anisotropic index quantifies the deviation from spatial homogeneity.The non-orthogonal tensor basis chosen is intuitively appealing since it is based on three simple, yet descriptive,geometrically meaningful cases.We have described how tensor diffusion data can be processed without reverting to the use of only scalar measures of the tensor data. By staying in the tensor domain, cleaning up of the data can be done meaningfully with simple methods such as smoothing.We discuss addition of tensors geometrically and argue that adding tensors and vectors are different in that tensor summation gives more than the ”mean” event due to more degrees of freedom.By using the geometric diffusion measures on locally averaged tensors local directionality consistency can be determined (e.g. existence of larger fiber tracts).We have proposed that this averaging approach can be used to derive a tensor field that can be used to describe macrostructural features in the tensor diffusion data.The linear measure cl derived from the averaged tensor field can for example be used for quantitative evaluation of fiber tract organization.We also have described how non-linear operations can be used to remap the eigenvalues of the diffusion tensors and given a sketch of how this can be used for tracking white matter tracts.

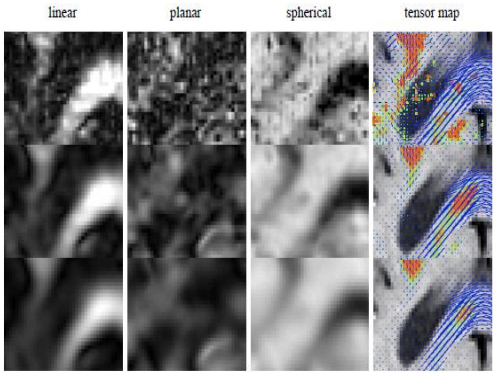

Fig.6.Axial brain images showing the three geometrical measures and diffusion tensor maps with three different smoothing parameters.

Top: shows the geometrical measures and the tensor map derived from the original data.

Middle: shows the same measures derived from data that has been averaged with 9x9x3 Gaussian kernel.

Bottom: from data averaged with a 15x15x5 Gaussian kernel. The rightmost column shows the tensors. The blue headless arrows represent the in-plane components of $c_l\vec{e}_1$The out-of-plane components of $c_l\vec{e}_1$(cl^e1) are shown in colors ranging from green through yellow to red, with red indicating the highest value for this component.

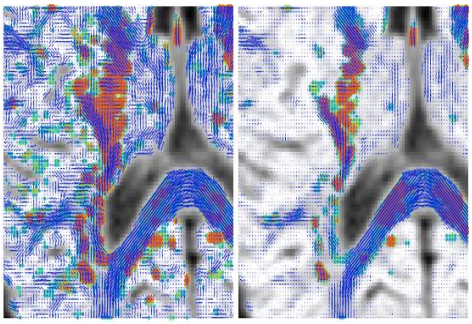

Figure 8.3. Left: Diffusion tensors, weighted with their linear measure c_l, from an axial slice of a human brain.Right: Averaged diffusion tensors using a 5x5x3 Gaussian kernel weighted with their linear measure c_l.

REFERENCES

[1] Alvarez, F. Guichard, P. L. Lions, and J. M. Morel, Axiomes et ´equations fondamentales du traitement d'images, C. R. Acad. Sci. Paris 315 (1992), 135–138.

[2] Axioms and fundamental equations of image processing, Arch. Rat. Mech. Anal. 123 (1993), no. 3, 199–257.

[3] Alvarez, P. L. Lions, and J. M. Morel, Image selective smoothing and edge detection by nonlinear diffusion, SIAM J. Numer. Anal. 29 (1992), 845–866.

[4] Alvarez and J-M. Morel, Formalization and computational aspects of image analysis,Acta Numerica3(1994),1–59.

[5] Ambrosio,A compactness theorem for a special class of functions of bounded variation,Boll.Un.Math.It. 3-B(1989),857–881.

[6] Lecture notes on optimal transport theory,Euro Summer School,Mathematical Aspects of Evolving Interfaces,CIME Series of Springer Lecture Notes, Springer,July 2000.

[7] S.Ando,Consistent gradient operators,IEEE Transactions on Pattern Analysis and Machine Intelligence 22(2000),no.3,252–265.

[8] S.Angenent,S.Haker,and A.Tannenbaum,Minimizing flows for the Monge Kantorovich problem, SIAM J. Math. Anal. 35 (2003), no. 1, 61–97 (electronic).

[9] S.Angenent,G.Sapiro,and A.Tannenbaum,On the affine heat flow for non-convex curves,J.Amer. Math. Soc. 11 (1998), no. 3, 601–634.

[10] J.-D. Benamou and Y. Brenier, A computational fluid mechanics solution to the Monge- Kantorovich mass transfer problem, Numerische Mathematik 84 (2000), 375–393.

[11] Mixed l2/wasserstein optimal mapping between prescribed density functions, J. Optimization Theory Applications 111 (2001), 255–271.

[12] Y. Brenier, Polar factorization and monotone rearrangement of vector-valued functions, Comm. Pure Appl.Math. 64 (1991), 375–417.

[13] D. Brooks, Emerging medical imaging modalities, IEEE Signal Processing Magazine 18 (2001), no. 6, 12–13.

[14] J. Canny, Computational approach to edge detection, IEEE Transactions on Pattern Analysis and Machine Intelligence 8 (1986), no. 6, 679–698.

[15] C-F. Westin, S. Peled, H. Gudbjartsson, R.Kikinis, and F.A Jolesz. Geometrical diffusion measures for MRI from tensor basis analysis. In *ISMRM '97*, Vancouver, Canada, April 1997.

[16] D. M.Wimberger, T. P. Roberts, A. J. Barkovich, L. M. Prayer,M. E.Moseley, and J. Kucharczyk. Identification of "premyelination" by diffusion-weighted MRI. *J. Comp. Assist. Tomogr*,19(1):28–33, 1995.

[17] H. Gudbjartsson, S. E. Maier, R. V. Mulkern, I. A´ . Mo´rocz, S. Patz, and F. A. Jolesz. Line scan diffusion imaging. *Magn. Reson. Med.*, 36:509–519, 1996.

[18] M. E. Moseley, Y. Cohen, J. Kucharczyk, J. Mintorovitch, H. S. Asgari, M. F. Wendland, J. Tsuruda, and D. Norman. Diffusion-weighted MR imaging of anisotropic water diffusion in the central nervous system. *Radiology*, 176:439–445, 1990.

[19] S. Peled, H. Gudbjartsson, C-F. Westin, R. Kikinis, and F.A. Jolesz. Magnetic Resonance Imaging shows Orientation and Asymmetry of White Matter Tracts. *Brain Research*, 780(1):27–33, January 1998.

[20] C. Pierpaoli, P. Jezzard, P. J. Basser, A. Barnett, and G. Di Chiro. Diffusion tensor MR imaging of the human brain. *Radiology*, 201:637, 1996.

[21] C. Poupon, J.-F. Mangin, F. Frouin, J. R´egis, F. Poupon, M. Pachot-Clouard, D. Le Bihan, and I. Bloch. Regularization of mr diffusion tensor maps for tracking brain white matter bundles. In *Proceedings of MICCAI'98*, number ISSN 0302-9743 in Lecture Notes in Computer Science 1496. Springer Verlag, 1998.

[22] R. Turner, D. le Bihan, J.Maier, R. Vavrek, L. K. Hedges, and J. Pekar.Echo planar imaging of intravoxel incoherent motions. *Radiology*, 177:407–414, 1990.

[23] C-F. Westin and H. Knutsson. Extraction of local symmetries using tensor field filtering.In *Proceedings of 2nd Singapore International Conference on Image Processing*.IEEE Singapore Section, September 1992.

[24] C-F.Westin and H. Knutsson. Estimation of Motion Vector Fields using Tensor Field Filtering. In *Proceedings of IEEE International Conference on Image Processing*, Austin, Texas, November 1994. IEEE

[25] L. C. Evans and J. Spruck, Motion of level sets by mean curvature, I, J. Differential Geometry 33 (1991), no. 3, 635–681.

[26] J.R. Fram and E.S. Deutsch, On the quantitative evaluation of edge detection schemes and their comparisons with human performance, IEEE Transaction on Computers 24 (1975), no. 6, 616–627.

[27] D. Fry, Shape recognition using metrics on the space of shapes, Ph.D. thesis, Harvard University, 1993.

[28] M. Gage and R. S. Hamilton, The heat equation shrinking convex plane curves, J. Differential Geometry 23 (1986), 69–96.

[29] W. Gangbo and R. McCann, The geometry of optimal transportation, Acta Math. 177 (1996), 113–161.

[30] E.S. Gerson, Scenes from the past: X-Ray mania, the X-Ray in advertising, circa 1895, Radiographics 24 (2004), 544–551.

[31] E. Giusti, Minimal surfaces and functions of bounded variation, Birkh¨auser Verlag, 1984.

[32] R. Gonzalez and R. Woods, Digital image processing, Prentice Hall, 2001.

[33] M. Grayson, The heat equation shrinks embedded plane curves to round points, J. Differential Geometry 26 (1987), 285–314.

[34] Shortening embedded curves, Annals of Mathematics 129 (1989), 71–111.

[35] F. Guichard, L. Moisan, and J.M. Morel, A review of PDE models in image processing and image analysis, Journal de Physique IV (2002), no. 12, 137–154.
[36] S.R. Gunn, On the discrete representation of the Laplacian of Gaussian, Pattern Recognition 32 (1999), no. 8, 1463–1472.
[37] J. Hajnal, D.J. Hawkes, D. Hill, and J.V. Hajnal (eds.), Medical image registration, CRC Press, 2001.
[38] S. Haker, L. Zhu, A. Tannenbaum, and S. Angenent, Optimal mass transport for registration and warping, Int. Journal Computer Vision 60 (2004), no. 3, 225–240.
[39] R. Haralick and L. Shapiro, Computer and robot vision, Addison-Wesley, 1992.
[40] S. Helgason, The Radon transform, Birkh¨auser, Boston, MA, 1980.
[41] W. Hendee and R. Ritenour, Medical imaging physics, 4 ed., Wiley-Liss, 2002.
[42] A.O. Hero and H. Krim, Mathematical methods in imaging, IEEE Signal Processing Magazine 19 (2002), no. 5, 13–14.
[43] R. Hobbie, Intermediate physics for medicine and biology (third edition), Springer, New York, 1997.
[44] B.K.P. Horn, Robot vision, MIT Press, 1986.
[45] G. Huisken, Flow by mean curvature of convex surfaces into spheres, J. Differential Geometry 20 (1984), 237–266.
[46] R. Hummel, Representations based on zero-crossings in scale-space, IEEE Computer Vision and Pattern Recognition, 1986, pp. 204–209.
[47] Radiology Centennial Inc., A century of radiology, http://www.xray.hmc.psu.edu/rci/centennial.html.
[48] Insight Segmentation and Registration Toolkit, http://itk.org.
[49] B. Julesz, Textons, the elements of texture perception, and their interactions, Nature 12 (1981), no. 290, 91–97.
[50] L. V. Kantorovich, On a problem of Monge, Uspekhi Mat. Nauk. 3 (1948), 225–226.
[51] S. Kichenassamy, A. Kumar, P. Olver, A. Tannenbaum, and A. Yezzi, Conformal curvature flows: from phase transitions to active vision, Arch. Rational Mech. Anal. 134 (1996), no. 3, 275–301.
[52] M. Knott and C. Smith, On the optimal mapping of distributions, J. Optim. Theory 43 (1984), 39–49.
[53] J. J. Koenderink, The structure of images, Biological Cybernetics 50 (1984), 363–370.
[54] W. K¨ohler, Gestalt psychology today, American Psychologist 14 (1959), 727–734.
[55] S. Osher L. I. Rudin and E. Fatemi, Nonlinear total variation based noise removal algorithms, Physica D 60 (1992), 259–268.
[56] H. Ishii M. G. Crandall and P. L. Lions, User's guide to viscosity solutions of second order partial differential equations, Bulletin of the American Mathematical Society 27 (1992), 1–67.
[57] A. Witkin M. Kass and D. Terzopoulos, Snakes: active contour models, Int. Journal of Computer Vision 1 (1987), 321–331.
[58] F. Maes, A. Collignon, D. Vandermeulen, G. Marchal, and P. Suetens, Multimodality image registration by maximization of mutual information, IEEE Transactions on Medical Imaging 16 (1997), no. 2, 187 – 198.
[59] J. Maintz and M. Viergever, A survey of medical image registration, Medical Image Analysis 2 (1998), no. 1, 1–36.
[60] S. Mallat, A wavelet tour of signal processing, Elsevier, UK, 1999.
[61] D. Marr, Vision, Freeman, san Francisco, 1982.
[62] D. Marr and E. Hildreth, Theory of edge detection, Proc. R. Soc. Lond. B (1980), no. 207, 187–217.
[63] R. McCann, A convexity theory for interacting gases and equilibrium crystals, Ph.D. Thesis, Princeton University, 1994.
[64] T. McInerney and D. Terzopoulos, Topologically adaptable snakes, Int. Conf. on Computer Vision (Cambridge, Mass), June 1995, pp. 840–845.
[65] Deformable models in medical image analysis: a survey, Medical Image Analysis 1(1996), no. 2, 91–108.
[66] J. Milnor, Morse theory, Princeton University Press, 1963.
[67] J-M. Morel and S. Solimini, Variational methods in image segmentation, Birkh¨auser, Boston, 1994.
[68] D. Mumford, Geometry-driven diffusion in computer vision, ch. The Bayesian Rationale for Energy Functionals, pp. 141–153, Kluwer Academic Publisher, 1994.
[69] D. Mumford and J. Shah, Boundary detection by minimizing functionals, IEEE Conference on Computer Vision and Pattern Recognition, 1985, pp. 22–26.
[70] Optimal approximations by piecewise smooth functions and associated variation problems, Comm. Pure Appl. Math. 42 (1989), no. 5, 577–685.
[71] S. Osher and R. P. Fedkiw, Level set methods: An overview and some recent results, Journal of Computational Physics 169 (2001), 463–502.
[72] S. J. Osher and J. A. Sethian, Front propagation with curvature dependent speed: Algorithms based on hamilton-jacobi formulations, Journal of Computational Physics 79 (1988), 12–49.
[73] Jacob Palis, Jr. and Welington de Melo, Geometric theory of dynamical systems, Springer- Verlag, New York, 1982, An introduction, Translated from the Portuguese by A. K. Manning.
[74] G.P. Penney, J. Weese, J.A. J.A. Little, P. Desmedt, D.L.O Hill, and D.J. Hawkes, A comparison of similarity measures for use in 2-D-3-D medical image registration, IEEE Transactions on Medical Imaging 17 (1998), no. 4, 586–595.
[75] P. Perona and J. Malik, Scale-space and edge detection using anisotropic diffusion, IEEE Trans. Pattern Anal. Machine Intel. 12 (1990), 629–639.
[76] E. Pichon, A. Tannenbaum, and R. Kikinis, Statistically based flow for image segmentation, Medical Imaging Analysis 8 (2004), 267–274.
[77] J.P.W Pluim and J.M. Fitzpatrick (Editors), Special issue on image registration, IEEE Transactions on Medical Imaging 22 (2003), no. 11.
[78] J.P.W Pluim, J.B.A. Maintz, and M.A. Viergever, Mutual-information-based registration of medical images: a survey, IEEE Transactions on Medical Imaging 22 (2003), no. 8, 986–1004.
[79] J. Sethian R. Malladi and B. Vemuri, Shape modeling with front propagation: a level set approach, IEEE Trans. Pattern Anal. Machine Intell. 17 (1995), 158–175.
[80] S. Rachev and L. R¨uschendorf, Mass transportation problems, Springer, 1998.
[81] L. Roberts, Optical and electro-optical information processing, ch. Machine perception of 3-D solids, MIT Press, 1965.
[82] W.C. Roentgen, Ueber eine neue Art von Strahlen, Annalen der Physik 64 (1898), 1–37.
[83] G. Sapiro, Geometric partial differential equations and image processing, Cambridge University Press, Cambridge, 2001.
[84] G. Sapiro and A. Tannenbaum, Affine invariant scale-space, International Journal of Computer Vision 11 (1993), no. 1, 25–44.
[85] On invariant curve evolution and image analysis, Indiana Univ. Math. J. 42 (1993),no. 3, 985–1009.
[86] On affine plane curve evolution, Journal of Functional Analysis 119 (1994), no. 1,79–120.
[87] J.A. Sethian, Levelset methods and fast marching methods, Cambridge University Press, 1999.
[88] K. Siddiqi, Y. Lauziere, A. Tannenbaum, and S. Zucker, Area and length minimizing flows for shape segmentation, IEEE TMI 7 (1998), 433–443.

[89] L. Simon, Lectures on geometric measure theory, Proceedings of the Centre for Mathematical Analysis, Australian National University, Canberra, 1983.
[90] 3D Slicer, http://slicer.org.
[91] I.E. Sobel, Camera models and machine perception, Ph.D. thesis, Stanford Univ., 1970.
[92] M. Sonka, V. Hlavac, and R. Boyle, Image processing: Analysis and machine vision, 2 ed. Brooks Cole, 1998.
[93] A. Toga, Brain warping, Academic Press, San Diego, 1999.
[94] A. Tsai, A. Yezzi, and A. Willsky, A curve evolution approach to smoothing and segmentation using the Mumford-Shah functional, CVPR (2000), 1119–1124.
[95] R. von de Heydt and E. Peterhans, Illusory contours and cortical neuron responses, Science 224 (1984), no. 4654, 1260–2.
[96] B. White, Some recent developments in differential geometry, Mathematical Intelligencer 11 (1989), 41–47.
[97] A. P. Witkin, Scale-space filtering, Int. Joint. Conf. Artificial Intelligence (1983), 1019–1021.
[98] L. Zhu, On visualizing branched surfaces: An angle/area preserving approach, Ph.D. thesis, Department of Biomedical Engineering, Georgia Institute of Technology, 2004.